

Magnetic resonance evaluation of spinal dysraphism in children

R. K. Gupta¹, A. Sharma², A. Jena¹, G. Tyagi², B. Prakash², and S. Khushu¹

¹ Nuclear Medicine Research Centre, Institute of Nuclear Medicine and Allied Sciences, Delhi, India

² Department of Neurosurgery, G. B. Pant Hospital, New Delhi-110002, India

Received November 30, 1988/Revised April 24, 1989

Abstract. Magnetic resonance (MR) imaging of the spine was performed as the initial imaging technique in 20 children when spinal dysraphism was suspected clinically and plain radiographs showed spina bifida. The correlation with surgical findings indicated that MR provided accurate information preoperatively in all the cases. Some unusual observations in cases with spina bifida cystica and occulta are discussed. It is concluded that plain radiograph and MR complete the preoperative radiologic evaluation of cases with spinal dysraphism.

Key words: Magnetic resonance imaging – Spinal dysraphism – Spinal cord abnormalities – Pediatric spinal cord

Spinal dysraphism designates the group of congenital abnormalities of the spine that involve, in part, imperfect fusion of midline mesenchymal, bony, and neural structures [13, 18]. The radiographic evaluation of pediatric spina bifida traditionally includes plain radiographs, myelography, and computed tomography (CT) [8, 13, 18]. These modalities are, however, associated with the risk of intrathecal contrast material and radiation exposure, and they require general anaesthesia in most patients [1, 2, 16]. Clinical experience with magnetic resonance (MR) in the diagnosis of spinal disorders is now well established [1–3, 6, 7, 10, 16]. Recently, MR has been prescribed as the initial diagnostic tool in the evaluation of spinal dysraphism due to its ability to perform multiplanar imaging and characterize the intraspinal contents without bony artefacts [1, 3, 10, 16].

The aim of this communication is to report some unusual and diverse MR findings of spinal dysraphism in children.

Patients and methods

Twenty children, ranging in age from 15 days to 14 years, with dysraphism were evaluated with MR. These children were referred for MR in order to evaluate spinal cord symptoms caused by the dysraphic condition. A plain radiograph of the spine was done in all cases prior to MR examination. Myelography and metrizamide CT were not performed because of their reported hazards and comparatively inferior resolution [1, 10, 16]. MR examinations were correlated with surgical findings in all cases.

MR was performed with a 1.5-T super-conducting MR scanner (Magnetom, Siemens). The spin-echo technique was used with an echo time (TE) of 28 ms and repetition time (TR) ranging from 500 to 700 ms, to obtain T1 weighted images. The slice thickness was 5 mm with no interslice interval. The images were obtained in sagittal, coronal, and axial planes on a 256 × 512 matrix. The upper cervical spine in sagittal plane was routinely studied in all these cases to look for the position and shape of the cerebellar tonsils and brain stem. When T2 weighted images were required, a double echo pulse sequence with a TE of 28 and 84 ms and a TR of 2800 ms was used. In patients younger than 5 years of age, routine sedation with oral chloral hydrate syrup, 50 mg/kg body weight, was given 30 min prior to the scan.

Results

The MR findings of the 20 patients are summarized in Table 1. MR examination in these cases included five cases of spina bifida cystica (SBC). Of the five children with SBC, three had cervical meningocele and two had lumbar meningocele. In all three cases with cervical meningocele, the spinal cord was tethered posteriorly by a thick band, biopsy material from this revealed fibrous tissue (Fig. 1). One case had Chiari I anomaly and another showed Chiari II anomaly with syringohydromyelia extending from the 2nd cervical to the 8th dorsal vertebrae. Of the two children with lumbar meningocele, one showed localized syrinx involving the 11th dorsal to the 1st lumbar vertebrae with a small septum partially dividing the cavity (Fig. 2). Tethered cord was seen in both the cases of lumbar meningocele.

Table 1. Summary of cases

Spinal dysraphism	Associated abnormalities							
	Meningocele	Syringohydromyelia	Band (fibrous)	Chiari malformation	Lipomyeloschisis	Diastematomyelia ^a	Lipomas	Low conus ^b (tethered cord)
Spina bifida cystica (<i>n</i> = 5)								
Cervical (<i>n</i> = 3)	3	1	3	2	–	–	–	–
Lumbar (<i>n</i> = 2)	2	1	–	–	–	–	–	2
Spina bifida occulta (<i>n</i> = 15)								
Dorsal (<i>n</i> = 2)	–	1	–	–	1	1	1	–
Dorsolumbar (<i>n</i> = 1)	–	3	–	–	–	–	–	–
Lumbar (<i>n</i> = 12)	–	1	1	–	7	7	5	2
Total	20	5	4	2	8	8	6	4

^a Three cases with diastematomyelia had syringohydromyelia near the superior end of the split cord

^b Five cases with diastematomyelia and all the cases with lipomyeloschisis also had low conus

Spina bifida occulta (SBO)

MR correctly identified abnormal spinal cord morphology in all the 15 cases. Spina bifida involving the lumbar spine was seen in the majority (*n* = 12), followed by dorsal (*n* = 2) and dorsolumbar spine (*n* = 1).

Tethered cord

The spinal cord was considered tethered when filum terminale was more than 1.5 mm thick and/or the conus was lower than the 2nd lumbar vertebral body [9]. Primary tethered cord was seen in two cases with lumbar spina bifida.

Diastematomyelia

Diastematomyelia was diagnosed when a split cord with dural penetration by a bony, cartilagenous or fibrous spur or merely a split cord with intact dural sleeves was seen [8]. There were eight cases with diastematomyelia. The bony septum was seen in three, fibrous septum in three, and splitting of cord without septum in the remaining two. The bony septum was identified as a continuation of bone marrow intensity with edges of the bone showing very low intensity on both T1 and T2 weighted images. The fibrous septum showed low intensity on both T1 and T2 weighted images. In these cases sagittal images showed some bands going from the posterior to the anterior part of the spine in the area that showed diastematomyelia on axial scan (Fig. 3). The axial scan was found to be ideal for demonstration of diastematomyelia, though the extent of the split cord could also be seen on coronal view. Three cases with diastematomyelia were associated with localized syringohydromyelia near the rostral end of the split cord (Fig. 3). Low conus was seen in five cases with diastematomyelia.

Lipomyeloschisis

Cord tethering to an intradural lipoma at the level of SBO was diagnosed as lipomyeloschisis [12]. This was seen in eight cases, seven of which had lumbar SBO. The conus was seen lying low in all the cases. The lipomatous tissue was seen extending upward and downward in-

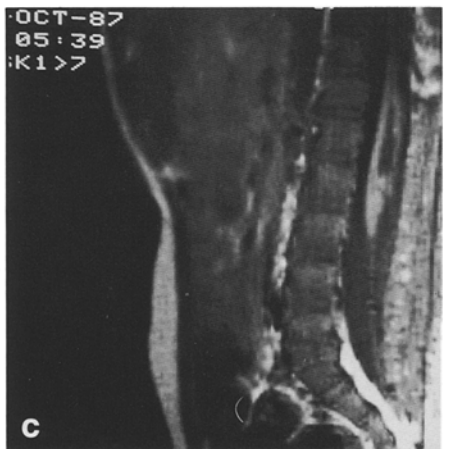
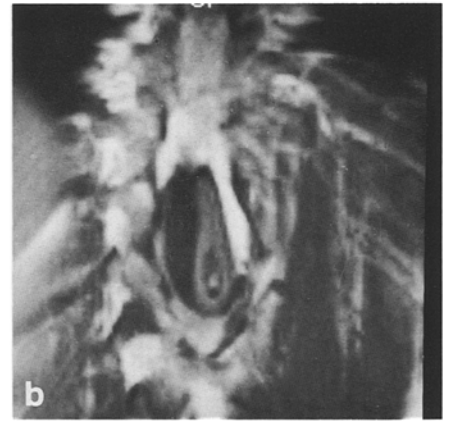
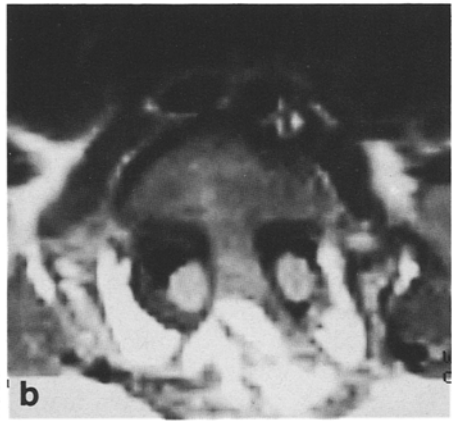
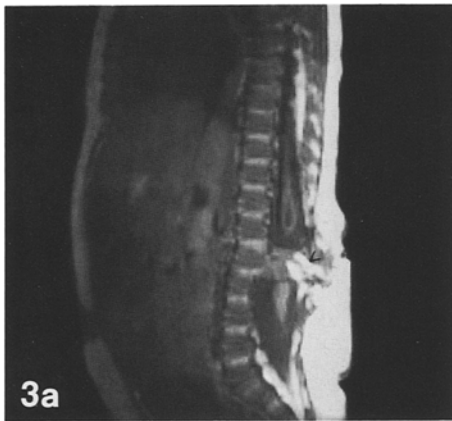
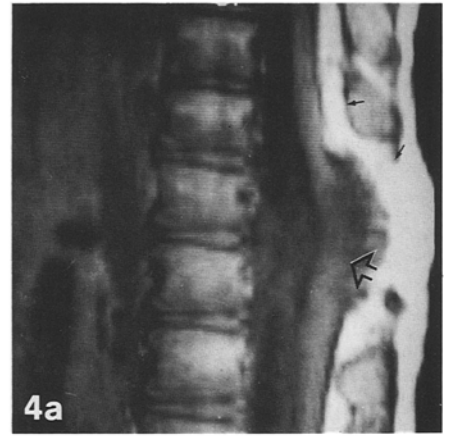
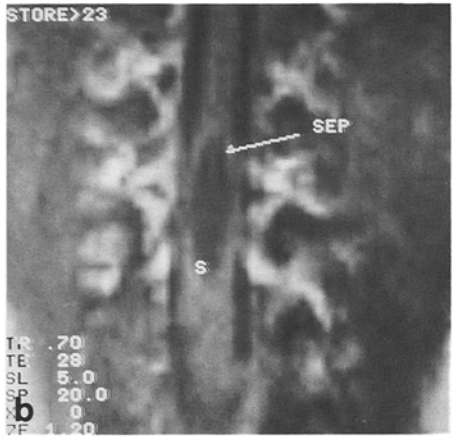
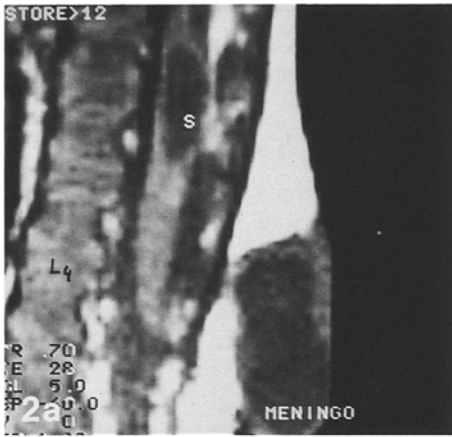
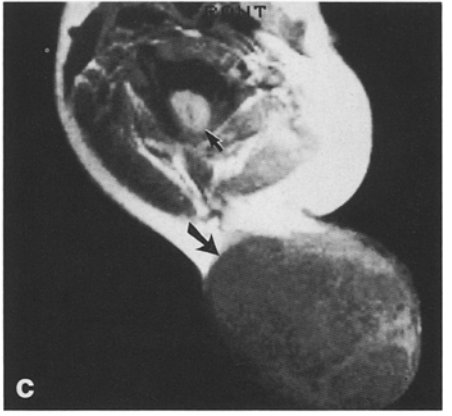
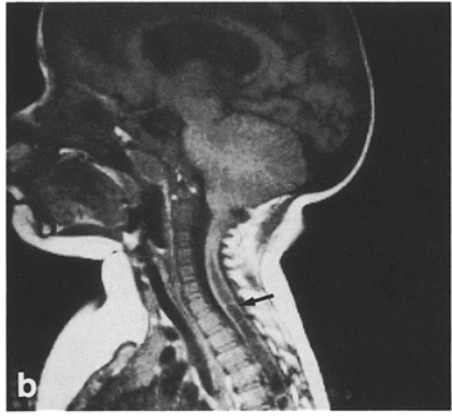
Fig. 1 a–c. Cervical meningocele with Chiari II malformation with tethered cord by fibrous band. **a** Sagittal T1 weighted MR demonstrates a band at the level of C2–3 pulling the spinal cord posteriorly. In addition, the associated Chiari II anomaly is demonstrated with low position of posterior fossa contents and hydrocephalus. **b** Right parasagittal T1 weighted MR demonstrates syringohydromyelia (*arrow*). **c** Axial T1 weighted MR at the level of C2–3 shows posteriorly placed tethered cord (*small arrow*) with meningocele (*large arrow*)

Fig. 2 a, b. Lumbar meningocele. **a** Sagittal T1 weighted MR demonstrates meningocele (*meningo*) and conus at L4. Note the syrinx (*S*) in the upper part of the cord. **b** Coronal T1 weighted MR shows a syrinx (*S*) with a small septum (*arrow*) in its rostral part

Fig. 3 a, b. Diastematomyelia with rostral syrinx. **a** Sagittal T1 weighted MR demonstrates a thick band of bone marrow intensity extending up to the posterior margin of L2 vertebral body. Posterior end of this band is covered by fat (*arrowhead*). The conus is seen at the level of L4. Note the syrinx rostral to the bony band, suggesting rostral end of the split cord. **b** Axial T1 weighted MR at the level of L2 shows bony septum completely splitting the cord. The low signal at the edge of the spur is due to cortical bone. Note the lipoma in the extradural space

Fig. 4 a, b. Dorsal lipomyeloschisis. **a** Sagittal T1 weighted MR shows lipoma extending from subcutaneous tissue into the spinal canal (*small arrows*). The intradural component of the fat is extending cranially. Note the tethering of the cord posteriorly (*open arrow*). **b** Coronal T1 weighted MR demonstrates the intramedullary lipoma tethering the cord. Note the dilatation of the central canal around the intramedullary component of lipoma

Fig. 5 a–c. Terminal syrinx with tethered cord. **a** Sagittal T1 weighted MR shows dilatation of the terminal part of the cord (*arrow*). **b** Coronal T1 weighted MR also demonstrates the dilatation of the central canal of the terminal portion of the cord. **c** Postoperative sagittal MR shows decrease in size of the syrinx



tradurally in five cases. In four cases, lipomyeloschisis was associated with diastematomyelia. In one patient with dorsal spina bifida, a component of lipoma grew upwards and within the central canal of the cord and ballooned it (Fig. 4).

Lipoma

The cases were grouped separately as lipoma when they were seen either as involving extradural space or subcutaneous tissue or as extending from subcutaneous tissue to extradural space. Subcutaneous with extradural lipoma was seen in five cases in lumbar dysraphism, of which two had diastematomyelia. Isolated extradural lipoma was seen in one case of dorsal dysraphism associated with diastematomyelia.

Syringohydromyelia

Syringohydromyelia was seen in five cases and was localized to a small segment of the spinal cord. One child had cystic dilation of the conus (Fig. 5). It has been differently described as ventriculus terminalis [3] and myelocystocele [1]. Cystosubarachnoid shunt was performed in this case. Postoperative MR showed a reduction in size but persistence of the lesion. Three cases with diastematomyelia were also shown to have localized syringohydromyelia near the rostral end of the split cord (Fig. 3).

Discussion

Spinal dysraphism represents a spectrum of congenital abnormalities with variable clinical and morphological presentation [13]. MR has become the technique of choice for evaluating the spine of children with suspected spinal dysraphism [1, 16]. It is reported that MR should be the initial screening procedure due to its ability to perform multiplanar imaging, tissue characterization, and show exquisite soft tissue details [10]. All the patients in this series were evaluated with MR and correlation was based on the surgical results.

SBC is designated by posterior protrusion of all or part of the spinal contents through a posterior spina bifida [13]. The meningocele and meningomyelocele of the lumbosacral region are most common in order of frequency, followed by cervical and dorsal spine, respectively [5]. In cases with Chiari II malformation, a meningomyelocele is a nearly constant accompanying feature [4, 12, 19]. However, the malformation may have either a meningocele or meningomyelocele [15]. We had five cases of SBC, of which three were cervical meningocele and two had lumbar meningocele. Of the three cases with cervical meningocele, Chiari I anomaly was seen in one and Chiari II malformation was seen in another. All three cases with cervical meningocele showed a tethering of cervical cord backward by a band. Biopsy material of this band was reported to be fibrous tissue. Occasionally, loops of herniated nerves are known to become adherent to the wall of the meningocele sac [13], but no fibrous

band has been reported so far. The meningocele and meningomyelocele are commonly associated with syringohydromyelia; it was seen in two out of five patients with SBC. In one patient with lumbar meningocele, localized syringohydromyelia was associated with a small septum running for a small distance. This type of abnormality has not been reported previously.

SBO is frequently an incidental finding on plain radiography. There is a small group of cases where an early diagnosis and surgery are most beneficial for the prevention of progressive disability [18]. Pathologically, tethering is due to or associated with tight, thick filum terminale, low conus, lipomyeloschisis, fibrous band, diastematomyelia, and neuroenteric or dermoid cysts [13, 18]. Hydromyelia is uncommon in lipomyeloschisis [14]. There were eight cases of lipomyeloschisis in the present series, two of which showed localized dorsal syrinx.

Han et al. [7] reported a case of diastematomyelia, with a syrinx near the superior end of the split cord and claimed that syringohydromyelia without Chiari malformation had not been cited in previous studies occurring with diastematomyelia. However, Schiffer and Till [17] described a case of diastematomyelia with a syrinx above the divided cord. Similar observations have also been made by Kuharik et al. [10]. We observed syrinx, rostral to the split cord, in three of eight cases of diastematomyelia and feel that the observation is not as uncommon as has been described. It is probably the ability of MR to detect smaller syringes that has made all the difference.

A localized cystic dilation of the spinal cord has been described as myelocystocele [11]. Altman and Altman [1] described myelocystocele as cystic dilation of the terminal portion of the spinal cord from cerebrospinal fluid (CSF) and differentiated it from a more proximal cystic dilation as hydromyelia. Delapaz et al. [3] described two cases with cystic dilation of the terminal portion of the cord and labelled them as dilated ventriculus terminus. We also observed cystic dilation of the terminal portion of the spinal cord by CSF in one case and feel that it should be designated as terminal syrinx. A differentiation between the myelocystocele and proximal hydromyelia has been made by showing drainage of myelocystocele via a lumbar cystoperitoneal shunt and persistence of hydromyelia [1]. It seems unusual that the myelocystocele containing CSF should not communicate with proximal syrinx unless there is some septum in between. In the present case, a cystosubarachnoid shunt was performed and postoperative MR showed reduction in size of the cystic cavity.

In conclusion, we feel that plain radiographs and MR form the complete radiologic work-up in the preoperative assessment of children with spinal dysraphism. Some observations, such as rostral syrinx associated with diastematomyelia, septum in the syrinx, fibrous band tethering the cervical cord with meningocele, and Chiari II malformation with cervical meningocele, were possible due to the better diagnostic abilities of MR. We feel that more frequent observations of these complex anomalies will become possible in the initial work-up performed using MR.

Acknowledgements. We acknowledge the assistance of Mr. Sitaram and Mrs. Shrilata Gupta in preparing this manuscript.

References

1. Altman NR, Altman DH (1987) MR imaging of spinal dysraphism. *AJNR* 8:533–538
2. Barness PD, Lester PD, Yamanishi WS, Prince JP (1986) Magnetic resonance imaging in infants and children with spinal dysraphism. *AJNR* 7:465–472
3. Delapaz RL, Floris R, Norman D, Newton TH (1986) MRI of tethered cord and caudal lipoma (abstract). *AJNR* 7:550
4. El Gammal T, Mark EK, Brooks BS (1987) MR imaging of Chiari II malformation. *AJNR* 8:1037–1044
5. Friede RL (1975) *Developmental neuropathology*. Springer, New York Berlin Heidelberg, pp 266–271
6. Han JS, Kaufman B, El Yousef SJ, Benson JE, Bonstelle CT, Alfidri RJ, Haaga JR, Yeung H, Huss RG (1983) NMR imaging of the spine. *AJR* 141:1137–1145
7. Han JS, Benson JE, Kaufman B, ReKate HL, Alfidri RJ, Bohlanman HH, Kaufman B (1985) Demonstration of diastematomyelia and associated abnormalities with MR imaging. *AJNR* 6:215–219
8. Harwood-Nash DC (1981) Computed tomography of the pediatric spine, a protocol for the 1980s. *Radiol Clin North Am* 19:479–494
9. Hochhouser L, Chaung S, Harwood-Nash DC, Fitz CR, Armstrong D, Savoie J (1986) The tethered cord syndrome revisited (abstract). *AJNR* 7:543
10. Kuharik MA, Edwards MK, Grossman CB (1986) Magnetic resonance evaluation of pediatric spinal dysraphism. *Pediatr Neurosci* 12:213–218
11. Lemire RJ, Loser JD, Leech RW, Alvord EC Jr (1975) Normal and abnormal development of the human nervous system. Harper & Row, Hagerstown, Md
12. McAdams AJ (1977) The Arnold Chiari malformation: pathology and developmental considerations. In: McLaurin RL (ed) *Myelomeningocele*. Grune & Stratton, New York, pp 197–207
13. Naidich TP, McLone DG, Harwood-Nash DC (1983) Spinal dysraphism. In: Newton TH, Pott DG (eds) *Computed tomography of the spine and spinal cord*. Clavadel Press, San Anselmi, Calif, pp 299–354
14. Naidich TP, McLone DG, Mutluer S (1983) A new understanding of dorsal dysraphism with lipoma (lipomyeloschisis): radiological evaluation and surgical correction. *AJNR* 4:103–116
15. Ramsey RG (1987) *Neuroradiology*. Saunders, Philadelphia, pp 440–441
16. Roos RAC, Vivelovoye GJ, Voormolen JHC, Petero ACB (1986) MR imaging in occult spinal dysraphism. *Pediatr Radiol* 16:412–416
17. Schiffer J, Till K (1982) Spinal dysraphism in the cervical and dorsal region in childhood. *Child's Brain* 9:73–84
18. Schut L, Pizzi FJ, Bruce DA (1977) Occult spinal dysraphism. In: McLaurin RL (ed) *Myelomeningocele*. Grune & Stratton, New York, pp 349–366
19. Wolpert SM, Anderson M, Scott RM, Kwan ESK, Runge VM (1987) The Chiari II malformation, MR imaging evaluation. *AJNR* 8:783–792